Silicate Cross-Linked Bio-Nanocomposite Hydrogels from PEO and Chitosan

Qu Jin, Patrick Schexnailder, Akhilesh K. Gaharwar, Gudrun Schmidt*

The compositions and the multi phase structures of bio-nanocomposite hydrogels made from silicate cross-linked PEO and chitosan are related to some of their physical and biological properties. The gels are injectable and self-healing because the cross-linking is physical and reversible under deformation. The presence of chitosan aggregates affects the viscoelastic properties and reinforces the hydrogel network. The chitosan adds advantageous properties to the hydrogel such as enhanced cell spreading and adhesion. *In vitro* biocompatibility data indicate that NIH 3T3 fibroblasts grow and proliferate on the bio-nanocomposite hydrogel as well as on hydrogel films.

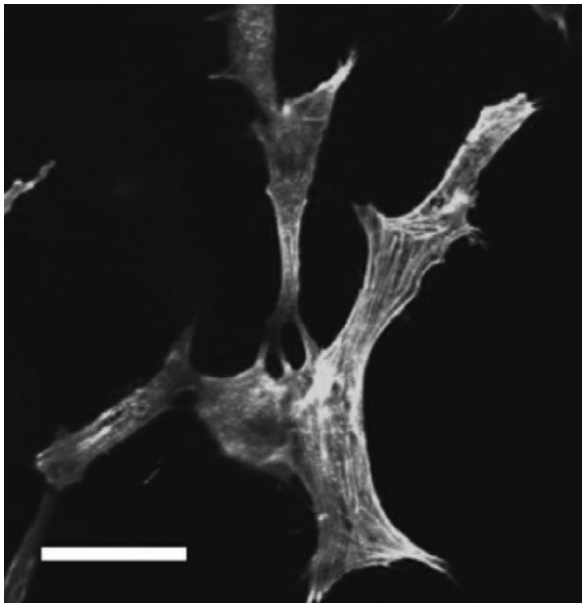

Introduction

Polymers, such as polysaccharides, proteins, and the combination of natural and synthetic polymers are increasingly used for improving the performance of materials for biomedical applications.[1] Natural polymers have advantageous properties over many synthetic polymers (e.g. biocompatibility, biodegradability).[2,3] However, disadvantages of natural polymers, including poor mechanical strength and potential immune system interactions, must be overcome for their continued and successful use in the biomedical field.[4]

Chitosan, a polycationic polymer composed of β-(1,4)-linked glucosamine subunits with randomly distributed *N*-acetylglucosamine subunits, is structurally similar to glycosaminoglycans. Chitosan is semicrystalline, but the crystallinity strongly depends on the degree of deacetylation.[5] Deacetylation affects mechanical properties as well as solubility. For example, highly deacetylated chitosans (50–90% deacetylation) are more soluble in water but degrade more slowly compared to low deacetylated chitosans.[6] The ability of chitosan to promote cell growth and maintain cellular phenotype, particularly of chondrocytes, makes this polysaccharide a desirable biomaterial for tissue engineering.[7,8] Chitosan derivatives may be used to inhibit fibroplasia in wound healing and promote ordered tissue reconstruction with little scar formation.[9] Solubility, thrombogenic and anticoagulant properties can be induced by chemically attaching functional groups to the chitosan backbone. Adhesive properties of cationic chitosan to tissue surfaces that have anionic groups are used for optimizing wound healing applications.[10] In addition, chitosan is enzymatically degraded by lysozyme, which is

Q. Jin, P. Schexnailder, A. K. Gaharwar, G. Schmidt
Weldon School of Biomedical Engineering, Purdue University, West Lafayette, IN 47907-2032, USA
Fax: +1 765 496 1912; E-mail: gudrun@purdue.edu

Macromol. Biosci. **2009**, *9*, 1028–1035

DOI: 10.1002/mabi.200900080

present in human body fluids.[5,6] The many uses of chitosan make it favorable for a broad variety of drug delivery formulations such as intra-tumoral administration[11] and specifically tailored biomedical applications.[7,9,12,13]

Synthetic and natural polymers can be used to synergistically combine the advantageous chemical, physical, and biological properties of the individual components to produce superior biomaterials. Our approach is predicated upon the development of a silicate cross-linked poly(ethylene oxide) (PEO) hydrogel containing chitosan. We have previously used silicate nanoparticles Laponite-RD (LRD) as reversible physical cross-linkers to PEO because the polymer readily adsorbs onto the nanoparticle surfaces.[14–18] The nanoparticles are synthetic and plate-like silicate polyions that form clear hydrogels with unique shear-thinning properties.[19–23] Successful formulations have strong specific interactions between LRD and PEO such as hydrogen bonding and ionic interactions.[24–29] The Laponite cross-linker can be purchased or synthesized and has been found to dissolve under certain pH-dependent conditions.[24,25]

As part of this work, we have investigated a series of bio-nanocomposite hydrogels that are both viscoelastic and injectable.[14–18] In order to reversibly cross-link the hydrogels at low polymer concentrations and to allow cell attachment and proliferation, we have used silicate nanoparticles to cross-link PEO hydrogels and chitosan to add biological properties of polysaccharides. While pure chitosan hydrogels often have poor mechanical properties and suffer from batch to batch variations, the bio-nanocomposite PEO/LRD/chitosan gels discussed below overcome some of these troubles because only low concentrations of chitosan are used. These hybrid gels should have mechanical properties that are dominated by the synthetic PEO polymer component whose synthesis does not pose problems with reproducibility. The chitosan thus adds all the advantageous properties mentioned above without hampering the mechanical strength of the hydrogel.

In the following text we discuss the multi phase structures of the gels and show how the structures relate to the viscoelastic properties. Then we present *in vitro* biocompatibility data showing that the presence of chitosan as well as the silicate nanoparticles within a PEO-based network allow for cell attachment, spreading, growth, and proliferation.

Experimental Part

Materials

Laponite RD from Southern Clay is a synthetic silicate consisting of nanoplatelets with diameter of 25–30 nm and thickness of about 1 nm. PEO with a $\overline{M}_w$ of 1 000 kg · mol^{-1} and a molecular mass distribution of ca. 1.5 was purchased from Polysciences Inc. Low-molecular-weight chitosan with 75–85% deacetylation was purchased from Sigma-Aldrich. The viscosity of a 1% chitosan solution with 1% acetic acid is 20–200 cP according to the provider. Rhodamine B ($\lambda_{Ex} = 540$ nm, $\lambda_{Em} = 625$ nm) was used as a fluorescent marker to the hydrogels. Alexa Fluor® 488 phalloidin ($\lambda_{Ex} = 495$ nm, $\lambda_{Em} = 518$ nm) was purchased from Invitrogen to stain F-actin. CellTiter 96® AQueous (Promega) was used for *in vitro* proliferation studies. Unless otherwise mentioned, all chemicals used were purchased from Sigma-Aldrich.

Preparation of Hydrogels and Films

2.5 wt.-% chitosan acidic solution was prepared by adding 2.5 g chitosan into 100 g of 0.1 M HCl. In separate containers, PEO and LRD were dissolved in de-ionized water, and the two solutions were combined to form gels. While stirring the LRD/PEO gels vigorously, chitosan and 0.1 M NaOH solutions were added to the gel drop by drop. The compositions of the final hydrogels are listed in Table 1. For *in vitro* biocompatibility tests, films were spread from the gels listed in Table 1. To obtain thicker films for better handling, several film layers were spread on top of each other, after the previous layers were dried. These films easily swelled in water to produce hydrogel films.

Digital Images of the Hydrogels

Hydrogels were transferred to glass bottom dishes and were covered with micro cover glass. The thickness of the hydrogel samples was 1.3 mm. The images showing transparency were taken with a digital camera.

Confocal Microscopy Observations

Confocal microscopy images were recorded on an Olympus Fluoview FV1000 confocal laser scanning microscope equipped with a 488 nm laser. Samples were observed using an Olympus UPLSAPO 20X objective lens. For evaluating the aggregation as function of chitosan concentration, the following procedure

Table 1. Sample names and compositions of LRD/PEO/Chitosan (LPChi) hydrogels and PEO (P) and LRD (L) controls in wt.-%.

Sample	Chitosan	PEO	LRD	H_2O
	wt.-%	wt.-%	wt.-%	wt.-%
L3P2Chi0	0	2	3	95
L3P2Chi0.2	0.2	2	3	94.8
L3P2Chi0.4	0.4	2	3	94.6
L3P2Chi0.6	0.6	2	3	94.4
P2	0	2	0	98
L3	0	0	3	97

was used: The flat background from the Laponite/Rhodamine B fluorescence was subtracted and the Fourier transformation of the images was done using a band pass filter to remove high and low frequency noise. A cumulative area fraction was obtained from the processed image and the shape of the aggregates was analyzed. A common compactness measure, called the circularity ratio, is defined as the ratio of the area of the shape to the area of a circle (the most compact shape) having the same perimeter. That ratio is expressed mathematically as $M = 4\pi$ (area)/(perimeter)^2. For a circle, the ratio is one and for an infinitely long and narrow shape, it is zero. We use the circularity ratio as a measure for the anisotropy of particles. Statistical analysis was performed using SAS version 9.1.3 (SAS Institute, Cary, NC) to determine statistical differences. A two sample *t*-test was performed using the Satterthwaite approximation due to unequal variances. $p < 0.01$ was deemed significantly different.

Rheological Tests

Rheological measurements were performed on an ARES strain-controlled rheometer (TA Instruments Ltd.) using a parallel plate geometry with 1 mm gap size. To test reproducibility, additional experiments were performed on an AR 2000 stress-controlled rheometer (TA Instruments Ltd.) using a 1° cone and plate geometry. For measuring the shear rate dependence of viscosity (performed at 25 °C), each point was recorded 5 min after the shear rate was applied. Strain dependent oscillatory shear experiments (frequency = 1 Hz) were performed at 25 and 37 °C. Hysteresis experiments were performed by subjecting the hydrogel to shear rates, from 1 to 567 s^{-1}, for 10 s per shear rate over a period of 2 min to generate the "up" curve. The samples were held at the maximum shear rate for 10 s before the shear rate was decreased back to 1 s^{-1} over a period of 2 min (10 s per shear rate) to generate the "down" curve. All rheological measurements were performed 30 min after the samples were loaded.

Cell Growth and Cell Adhesion Tests

Films made from hydrogels were sterilized by brief immersion into 70% ethanol and dried. Afterwards NIH 3T3 cells (ATCC) were seeded on hydrogels and on swollen hydrogel films at a density of 7 500 cells · cm^{-2} in 24-well tissue culture plates. Cells were cultured in Dulbecco's modified eagle's medium (DMEM) supplemented with 10% bovine calf serum, 4×10^{-3} M L-glutamine, 100 U · mL^{-1} penicillin and 100 μg · mL^{-1} streptomycin and incubated in 5% CO_2 at 37 °C. Media was changed every third day. Cells were fixed and stained following the manufacturer's protocol (Invitrogen). Briefly, the samples were fixed with 3.7% formaldehyde/PBS solution for 10 min. F-actin was stained with Alexa Fluor® 488 phalloidin (5 U · mL^{-1}) for 20 min. The morphology of the cells on the hydrogels and films was observed using an Olympus Fluoview FV1000 confocal laser scanning microscope. 1, 4, 7, 11, 14, 18, 21 d after seeding, [3-(4,5-dimethylthiazol-2-yl)-5-(3-carboxymethoxyphenyl)-2-(4-sulfophenyl)-2H-tetrazolium] MTS assays were performed following the manufacturer's protocol for CellTiter 96® Aqueous One solution cell proliferation assay. Briefly, the tissue culture plates containing samples were incubated in 5% CO_2 at 37 °C for 2 h after adding 100 μL MTS into 500 μL media for each of the wells. A SpectraMax M5 microplate reader was used to read the 96-well plates at $\lambda = 490$ nm. Cell proliferation on films was obtained by comparing the absorption to a standard curve. Error bars represent a standard error of mean value ($n = 4$).

Results and Discussion

Our previous and current research data suggest that it is possible to design silicate cross-linked PEO/chitosan hydrogels with a spectrum of viscoelastic properties for pathogen free, antimicrobial (chitosan) and non-fouling (PEO) biomedical use.[14–18,30,31] The silicate cross-linked PEO hydrogels are adhesive to tissue, have a soft and rubbery consistency, and can be made injectable.[17,18] The addition of chitosan improves the hydrogel matrix for cellular function.[7,8] Incorporation of silicate and chitosan into the PEO hydrogel may thus be used to enhance cell adhesion, growth, and proliferation.[32] We proceed by presenting results on the structure and viscoelastic properties of selected nanocomposite hydrogels with different chitosan compositions. Then we present results from *in vitro* biocompatibility studies. Taken together, these data provide a range of macroscopic gel stability and clues for improvement of hydrogel formulations to be considered as injectable biomaterials.

Structure and Viscoelastic Properties

Figure 1 summarizes results obtained from the structural characterization of the hydrogels investigated here. Digital images suggest that the optical clarity of the samples is inversely proportional to the concentration of incorporated chitosan (Figure 1A). For example, the sample with 0 wt.-% of chitosan is transparent to the eye, the sample with 0.2 wt.-% chitosan is highly translucent and the sample with 0.6 wt.-% chitosan is less translucent. The decrease in optical transparency suggests the presence of μm size particles or aggregates that scatter light. These aggregates form when the clear chitosan solution is vigorously mixed with the PEO-LRD solution at physiological conditions (pH = 7.4 and 37 °C). At a pH ≈ 7, Laponite nanoplatelets have negatively charged faces and positively charged edges.[24] The pK_a value of chitosan is 6.5–7.3. Thus chitosan is positively charged at pH values below this range, but the pK_a values are dependent on the degree of deacetylation.[33] If a PEO/LRD/chitosan sample is prepared at a pH below the pK_a, interactions between the charged chitosan molecules and the PEO coated LRD nanoparticles lead to aggregation and phase separation. Macroscopic phase separation and sedimentation of chitosan aggregates are suppressed because the particles are trapped within a three-dimensional hydrogel network. Increased heterogeneity in chitosan particle distribution as well as PEO clustering leads

DOI: 10.1002/mabi.200900080

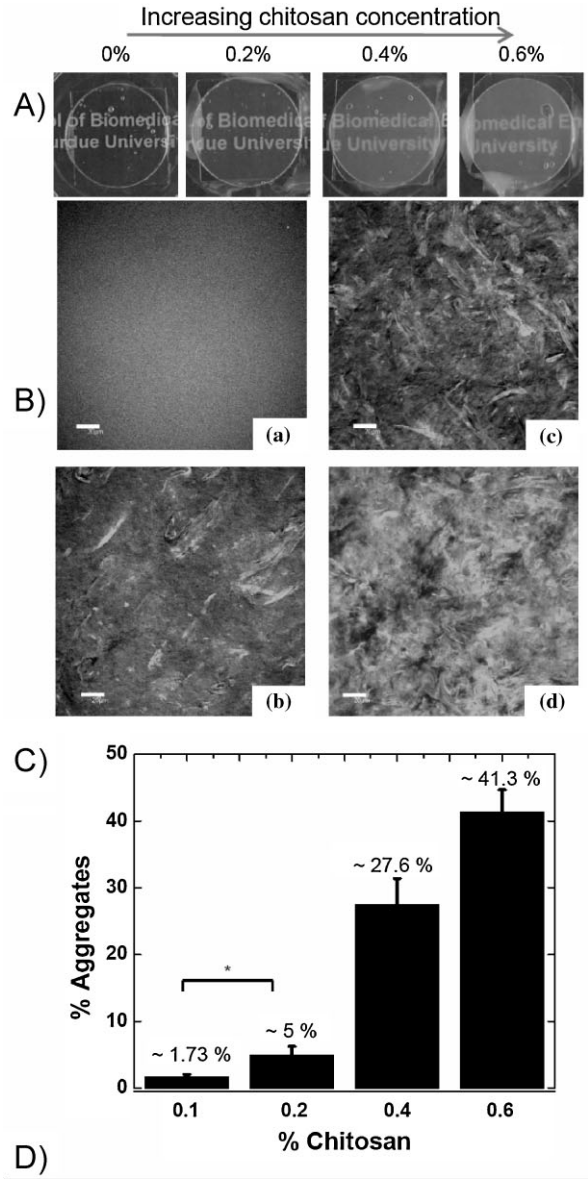

Chitosan (%)	0.1	0.2	0.4	0.6
Circularity	0.911 ± 0.002	0.876 ± 0.02	0.850 ± 0.006	0.846 ± 0.002

Figure 1. (A) The optical clarity of the hydrogels is inversely proportional to the concentration of chitosan. (B) Confocal microscopy of: (a) L3P2Chi0, (b) L3P2Chi0.2, (c) L3P2Chi0.4, (d) L3P2Chi0.6. Scale bar represents 20 μm. (C) Cumulative area fraction for different chitosan concentrations calculated from the inverted images by image analysis (Image J, NIH). Error bars represent the standard deviation computed from three different samples. All data are significantly different from each other ($p < 0.01$) except 0.1% and 0.2% which are different at the $p < 0.05$ level. (D) As the chitosan concentration increases, the circularity ratio (anisotropy) decreases, indicating that chitosan is mainly responsible for forming elongated (fiber-like) aggregates.

to increased turbidity. Confocal microscopy is used to visualize aggregates that were labeled with rhodamine B (Figure 1B). This fluorescent dye preferentially attaches to chitosan molecules through primary and secondary amine and hydroxyl functional groups[34] and allows for determining of number, size, and shape of aggregates. According to Grauer et al.[35] the dye also interacts with the Laponite nanoparticles, thus weakening the overall contrast as seen by the presence of a flat background for the reference PEO/LRD sample. Regardless, the number of the μm-scale aggregates visible in Figure 1B is strongly related to the concentration of chitosan. Application of the NIH Image J software enables assessment of the amount of aggregates from the confocal microscopy images. With increasing chitosan concentration, the amount of aggregation increases from 1.73% for 0.1% chitosan to 41.3% for 0.6% chitosan gels (Figure 1C). The shape of the μm-scale aggregates is found to be elongated and at times fiber-like which is possibly due to the mixing procedures (currently under investigation). The confocal microscopy image of the hydrogel with 0.6 wt.-% chitosan (Figure 1D) suggests overlapping aggregates at this composition.

On a nanometer length scale, preliminary small angle X-ray scattering studies (data not shown) indicate that scattering intensities decrease as a function of momentum transfer q and no characteristic features (peak or shoulder) are visible over a q-range of 0.006–0.15 $Å^{-1}$ (characteristic dimension $d = 4.2$–104.7 nm). Attempted Guinier analysis of the low-q data suggests the presence of aggregates in the range of 900, 1 750, and 2 500 nm in gels with chitosan concentrations of 0, 0.2, and 0.6 wt.-%. These "aggregates" do not necessarily correspond to pure chitosan aggregates but may consist of solution components including PEO and LRD. No further formulation is necessary to maintain gel stability and injectability of hydrogels at the concentrations investigated.

In the following we investigate the influence of chitosan on the viscoelastic properties of our hydrogels. The knowledge of these properties is important to maintaining injectability, developing self-healing properties, and easy processing. Similar to previous studies of reference PEO/LRD type gels,[14] shear thinning is observed for a series of chitosan containing PEO/LRD hydrogels over a wide range of shear rates ($d\gamma/dt$) (Figure 2A). The physically cross-linked hydrogel network containing chitosan will shear thin into low viscous gels under deformation, a property that makes them injectable via syringe. After cessation of shear, the network structure recovers and the rigidity of the hydrogel is restored immediately. The PEO/LRD reference sample shear thins and shows power law behavior over nearly all shear rates measured. The 3 wt.-% LRD control is also a shear thinning hydrogel, and the 2 wt.-% PEO control solution behaves like a Newtonian fluid (Figure 2A). Power law behavior is observed for all PEO/LRD/Chitosan samples.

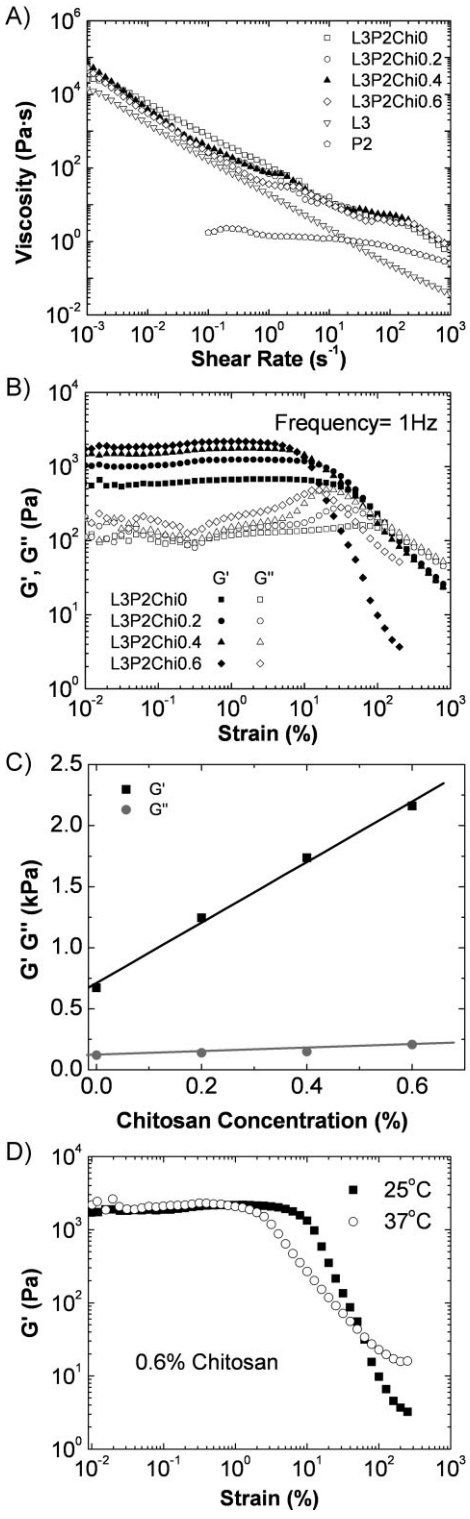

Figure 2. (A) Steady state viscosity as a function of shear rate for: L3P2Chio, L3P2Chio.2, L3P2Chio.4, L3P2Chio.6, PEO control, and LRD control. (B) Strain dependent elastic (G') and viscous moduli (G'' at 25 °C and at 1 Hz. (C) Linear dependence of G' and G'' with chitosan concentration. The moduli shown in (C) are obtained from data in (B) at 1% strain and 1 Hz. (D) G' of 0.6% chitosan sample at 25 and 37 °C.

At higher shear rates, viscosity values are higher compared to the LRD reference, which is due to polymer nanoparticle interactions. Within the PEO/LRD/Chitosan series, the 0.6% chitosan containing gel has lower viscosities compared to the rest of the hydrogels. Viscosities are slightly decreased by the addition of chitosan at low shear rates, but the viscosity of chitosan containing hydrogels do not significantly change at higher shear rates when compared to the viscosity of the reference PEO/LRD hydrogel. The presence of chitosan containing particles or aggregates must disrupt the PEO/LRD network under shear and decrease the viscosity within the series (Figure 2). Thus the addition of chitosan leads to some changes in the shear rate dependent viscosity behavior of PEO/LRD gels.

Figure 2B and C summarize strain dependent oscillatory shear experiments performed at 25 °C and a frequency of 1 Hz. The influence of chitosan concentration on viscoelastic moduli is clearly visible. All hydrogels show chitosan dependent viscoelastic plateaus up to strains of 10%. At low deformations, the elastic moduli G' are always larger than G'', and G′ increases with chitosan concentration (Figure 2B). The cross-over strains and cross-over moduli ($G' = G''$) are also dependent on the concentration of chitosan. Figure 2C shows that the elastic and viscous moduli of the hydrogels are linearly dependent on chitosan concentration. Overall, hydrogels with higher chitosan concentrations have smaller cross-over strains and larger cross-over moduli. These results suggest that adding chitosan to the gel decreases the strain above which the gel starts to flow. The presence of chitosan containing aggregates must disrupt the viscoelastic PEO/LRD network under shear and decrease the strain above which the overall sample yields. The strain distribution is expected to be locally non-uniform and dependent on the position of the chitosan aggregates within the gel. In addition, chitosan containing particles or fibers may enhance the elastic modulus by their rigidity while the PEO chains within the silicate cross-linked network are expected to be more flexible and stretch during deformation. Thus the hydrogel elasticity is probably influenced by both, enthalpy and entropy effects.[36] Viscoelastic parameters of the hydrogels at 25 and 37 °C are listed in Table 2, which include G' and G'' within the viscoelastic plateaus, cross-over strains, and stresses (yield stresses). Increasing the temperature from 25 to 37 °C slightly increases the value of the elastic modulus in the viscoelastic plateau (Figure 2D) but shortens the viscoelastic region that can be measured. At 37 °C, the hydrogel starts to flow at strains that are ca. 5–10% smaller than the strain measurements at 25 °C, an observation that leads to better injectability of gels at high temperatures (Table 2).

Macrostructural changes and recovery within hydrogel samples can be estimated by hysteresis experiments. In these experiments, the shear rate is increased to a maximum followed by decreasing the shear rate back to the

Macromol. Biosci. **2009**, *9*, 1028–1035

Macromolecular Journals
DOI: 10.1002/mabi.200900080

Table 2. Summary of G', G'' in the viscoelastic plateau, cross-over strains from strain sweep experiments (at 1 Hz frequency), and cross-over stresses from stress sweep experiments (not shown here) at 25 and 37 °C. Cross-over strains ($G' = G''$) were measured at 1 Hz, and cross-over stresses were measured at a strain of 1%.

Temperature	Sample	G'	G''	Cross-over strain	Cross-over stress
°C		Pa	Pa	%	Pa
25	L3P2Chi0	668	118	175.3	271.8
	L3P2Chi0.2	1 240	140	143.2	25.4
	L3P2Chi0.4	1 740	150	69.2	69.4
	L3P2Chi0.6	2 170	209	17.7	58.7
37	L3P2Chi0	844	146	125.8	158.7
	L3P2Chi0.2	1 490	160	25.2	5.4
	L3P2Chi0.4	2 010	163	13.8	22.2
	L3P2Chi0.6	2 080	256	6.32	17.3

starting value at a constant ramp rate while measuring the sample viscosity.[37] The area between the "up" and "down" curves indicates the hysteresis of the sample.[38] As the shear rate increases, network structures within the hydrogel progressively break down. These structures can begin to reform as the shear rate decreases.[38] Therefore, a decrease in area between the hysteresis curves serves as an indicator for how quickly the network structure reforms after deformation, an important factor for injectable materials. Figure 3 shows the results of hysteresis experiments on L3P2 hydrogels with increasing chitosan concentration. The area of hysteresis loops decreases with increase in chitosan concentration. This indicates that the presence of chitosan within the hydrogel samples decreases the time needed for recovery of the network. The increased recovery may be related to PEO/LRD/chitosan interactions at higher chitosan concentrations, which promote self-healing within this system.

Cell Growth Studies

Figure 4 summarizes cell growth studies showing cell morphologies on surfaces of hydrogels and hydrogel films (Figure 4A) and growth rates measured on hydrogel films (Figure 4B). MTS assays were used to evaluate the growth rate of fibroblast cells grown on the surfaces of hydrogel films (Figure 4). The number of cells on gel films was quantified 1, 4, 7, 11, 14, 18, and 21 d after seeding and plotted as function of time (Figure 4). Overall, fibroblast cells were found to proliferate on the hydrogel films showing little difference in cell growth between bio-nanocomposite and tissue culture polystyrene (TCPS) controls.

Figure 4 shows the morphology of NIH 3T3 fibroblasts on the surface of hydrogels (a and b) as compared to swollen hydrogel films (c and d) 24 h after seeding. The cells seeded on hydrogels without chitosan show round morphology, while the cells seeded on hydrogels containing chitosan spread out more with increase in number of filopodia (white arrows). The circumference or area of cells spread on hydrogels containing chitosan (b) seems larger than that on hydrogels without chitosan (a). While the stiffness of a substrate has been found to affect the spreading of cells[39]

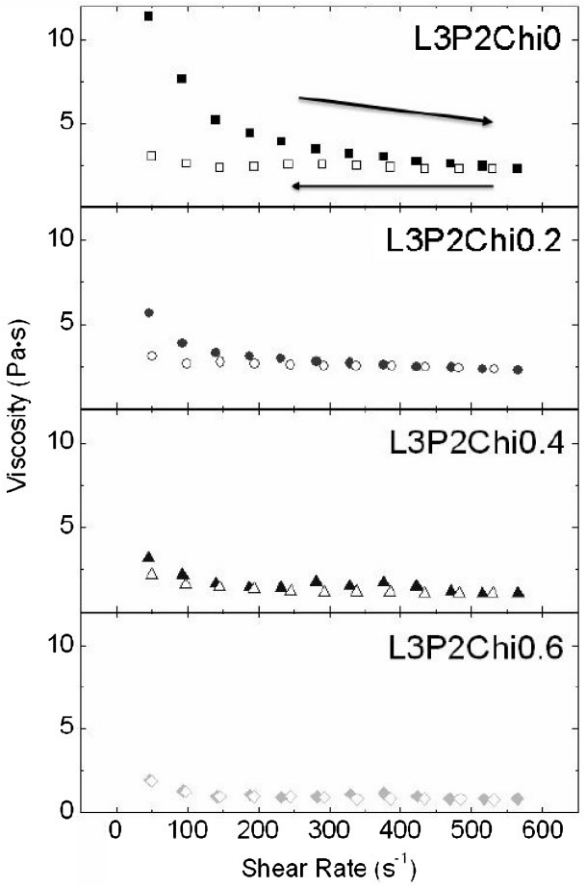

Figure 3. Hysteresis data for hydrogels listed in Table 1.

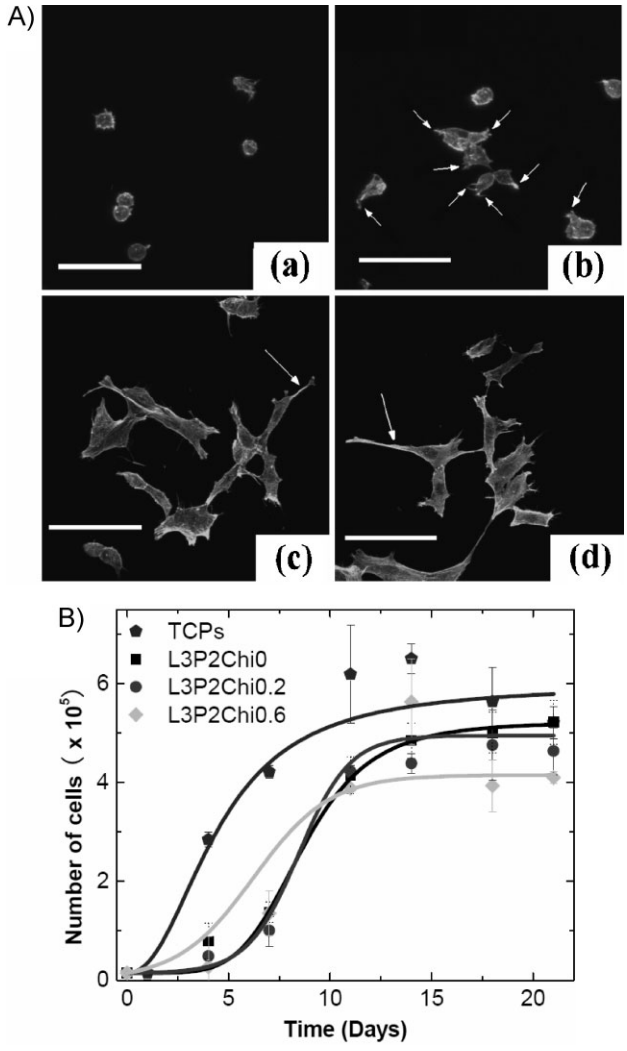

Figure 4. (A) Cell morphology on hydrogels and on (dried and re-swollen) hydrogel films as observed with confocal microscopy: (a) L3P2Chio hydrogel, (b) L3P2Chio.6 hydrogel, (c) L3P2Chio swollen hydrogel film, and (d) L3P2Chio.6 swollen hydrogel film. Cells were stained with phalloidin. The scale bars represent 100 μm. The arrows in (b) point to the filopodia spread out by the cells. (B) Number of NIH 3T3 cells on hydrogel films as function of time. Gel films were made from dried and re-swollen L3P2Chio, L3P2Chio.2, L3P2Chio.4, and L3P2Chio.6 hydrogels. Sigmoidal growth curve Boltzmann fittings are plotted as a guide to the eye.

Yeung et al.[40] showed that the circumference of NIH 3T3 fibroblasts does not change much when the modulus of fibronectin-coated substrates was increased from 10 to 2 500 Pa. Since the elastic moduli of the L3P2Chi0 and L3P2Chi0.6 hydrogels investigated here are within this range (Table 2), hydrogel stiffness should not significantly affect cell spreading. Thus differences observed in cell spreading must be due to the presence of chitosan, which is adhesive to cells.

The cell morphology and density observed for the hydrogel films is more or less similar on all gel film surfaces. Representative confocal microscopy images show cells attached and spread on the PEO/LRD control and PEO/LRD/chitosan film surfaces (c and d). No addition of proteins, other than proteins contained in calf serum, were necessary for cells to adhere to the nanocomposite films. The increased adhesion of cells on the surface of the swollen hydrogel films compared to that of the hydrogels may be due to differences of stiffness and composition. We assume that the swollen hydrogel films do not have the same composition (water content) as the hydrogels they were made from.

The ability to prevent protein denaturation and its non-toxicity makes these PEO-modified materials biocompatible for supporting cell growth.[41] While cells do not attach to pure PEO,[42] the combination of PEO, LRD, and chitosan leads to nanocomposite hydrogel materials with synergistic properties that allow cell attachment.

Conclusion

Overall, the data presented in this study provide a range of macroscopic stability for the hydrogels investigated. The composition and multi phase structures within the hybrid gels made from PEO, Laponite, and chitosan can be related to their viscoelastic properties. The μm sized chitosan particles and aggregates are well dispersed throughout the hydrogel matrix. These structures are trapped within the three-dimensional hydrogel network which inhibits their diffusion but reinforces the overall hydrogel network and affects shear thinning.

In vitro biocompatibility data indicate that NIH 3T3 fibroblasts readily adhere, grow, and proliferate on the bio-nanocomposite materials that we have investigated. While these preliminary *in vitro* studies suggest biocompatibility of our hydrogels, further development for long-term biomedical use will have to consider additional formulation and optimization to closely match the structural and mechanical properties of specific applications of interest. Our data on the above hydrogels suggest that it is possible to design hydrogels that might be formulated toward pathogen free, antimicrobial (chitosan), and non-fouling (PEO) biomedical use.[14–18,30,31]

Acknowledgements: This research has been supported in part by an *NSF CAREER award* DMR-0711783 to GS and by a *Purdue Lynn Doctoral fellowship* to PS. We thank Mr. *Patrick Downs* and Ms. *Ashmita Hoskote* for assistance with sample preparation and rheology experiments. We thank Professor Alyssa Panitch for letting us use her plate reader and Dr. Mikhail Slipchenko and Shuhua Yue from Professor Ji-Xin Cheng's group for showing QJ how to use the confocal microscope.

Received: February 17, 2009; Revised: May 1, 2009; Accepted: May 5, 2009; Published online: July 10, 2009; DOI: 10.1002/mabi.200900080

Keywords: chitosan; hydrogels; polymers; rheology; silicates

Macromol. Biosci. **2009**, *9*, 1028–1035

DOI: 10.1002/mabi.200900080

[1] P. X. Ma, *Mater. Today* **2004**, *7*, 30.
[2] L. S. Nair, C. T. Laurencin, "*Tissue Engineering I: Scaffold Systems for Tissue Engineering*", K. Lee, D. Kaplan, Eds., Springer, Heidelberg 2006, p. 47.
[3] P. Schexnailder, G. Schmidt, *Colloid Polym. Sci.* **2009**, *287*, 1.
[4] F. Causa, P. A. Netti, L. Ambrosio, *Biomaterials* **2007**, *28*, 5093.
[5] T. Freier, H. S. Koh, K. Kazazian, M. S. Shoichet, *Biomaterials* **2005**, *26*, 5872.
[6] S. Hirano, H. Tsuchida, N. Nagao, *Biomaterials* **1989**, *10*, 574.
[7] V. F. Sechriest, Y. J. Miao, C. Niyibizi, A. Westerhausen-Larson, H. W. Matthew, C. H. Evans, F. H. Fu, J. K. Suh, *J. Biomed. Mater. Res.* **2000**, *49*, 534.
[8] J. X. Lu, F. Prudhommeaux, A. Meunier, L. Sedel, G. Guillemin, *Biomaterials* **1999**, *20*, 1937.
[9] R. A. A. Muzzarelli, *Carbohydr. Polym.* **1993**, *20*, 7.
[10] A. Chenite, C. Chaput, D. Wang, C. Combes, M. D. Buschmann, C. D. Hoemann, J. C. Leroux, B. L. Atkinson, F. Binette, A. Selmani, *Biomaterials* **2000**, *21*, 2155.
[11] E. Ruel-Gariépy, M. Shive, A. Bichara, M. Berrada, D. Le Garrec, A. Chenite, J. C. Leroux, *Eur. J. Pharm. Biopharm.* **2004**, *57*, 53.
[12] E. Ruel-Gariepy, J. C. Leroux, "*Symposium on Polysaccharides for Drug Delivery and Pharmaceutical Applications held at the 228th ACS National Meeting*", R. H. Marchessault, F. Ravenelle, X. X. Zhu, Eds., American Chemical Society, Washington 2006, p. 243.
[13] E. Wagner, J. Kloeckner, "*Polymer Therapeutics I: Polymers as Drugs, Conjugates and Gene Delivery Systems*", R. Satchi-Fainaro, R. Duncan, Eds., Springer, Berlin 2006, p. 135.
[14] G. Schmidt, A. I. Nakatani, P. D. Butler, C. C. Han, *Macromolecules* **2002**, *35*, 4725.
[15] G. Schmidt, A. I. Nakatani, P. D. Butler, A. Karim, C. C. Han, *Macromolecules* **2000**, *33*, 7219.
[16] G. Schmidt, A. I. Nakatani, C. C. Han, *Rheologica Acta* **2002**, *41*, 45.
[17] E. Loizou, P. Butler, L. Porcar, E. Kesselman, Y. Talmon, A. Dundigalla, G. Schmidt, *Macromolecules* **2005**, *38*, 2047.
[18] E. Loizou, P. Butler, L. Porcar, G. Schmidt, *Macromolecules* **2006**, *39*, 1614.
[19] J. D. F. Ramsay, *J. Colloid Interface Sci.* **1986**, *109*, 441.
[20] J. D. F. Ramsay, P. Lindner, *J. Chem. Soc. Faraday Trans.* **1993**, *89*, 4207.
[21] J. D. F. Ramsay, S. W. Swanton, J. Bunce, *J. Chem. Soc. Faraday Trans.* **1990**, *86*, 3919.
[22] F. Pignon, A. Magnin, J. M. Piau, B. Cabane, P. Lindner, O. Diat, *Phys. Rev. E* **1997**, *56*, 3281.
[23] F. Pignon, J. M. Piau, A. Magnin, *Phys. Rev. Lett.* **1996**, *76*, 4857.
[24] D. Thompson, J. Butterworth, *J. Colloid Interface Sci.* **1992**, *151*, 236.
[25] V. Castelletto, I. A. Ansari, I. W. Hamley, *Macromolecules* **2003**, *36*, 1694.
[26] F. Cousin, V. Cabuil, P. Levitz, *Langmuir* **2002**, *18*, 1466.
[27] J. Zebrowski, V. Prasad, W. Zhang, L. Walker, D. Weitz, *Colloids Surf., A* **2003**, *213*, 189.
[28] D. Pozzo, L. Walker, *Colloids Surf., A* **2004**, *240*, 187.
[29] H. Baghdadi, H. Sardinha, S. Bhatia, *J. Polym. Sci., Part B: Polym. Phys.* **2005**, *43*, 233.
[30] S. H. Lee, J. S. Miller, J. J. Moon, J. L. West, *Biotechnol. Prog.* **2005**, *21*, 1736.
[31] S. H. Lee, J. J. Moon, J. S. Miller, J. L. West, *Biomaterials* **2007**, *28*, 3163.
[32] T. Uragami, S. Tokura, "*Materials Science of Chitin and Chitosan*", Springer, Heidelberg 2006.
[33] P. Sorlier, A. Denuziere, C. Viton, A. Domard, *Biomacromolecules* **2001**, *2*, 765.
[34] S. K. Das, P. Ghosh, I. Ghosh, A. K. Guha, *Colloids Surf., B* **2008**, *65*, 30.
[35] Z. Grauer, A. B. Malter, S. Yariv, D. Avnir, *Colloids Surf.* **1987**, *25*, 41.
[36] M. L. Gardel, J. H. Shin, F. C. MacKintosh, L. Mahadevan, P. Matsudaira, D. A. Weitz, *Science* **2004**, *304*, 1301.
[37] J. Greener, R. W. Connelly, *J. Rheol.* **1986**, *30*, 285.
[38] H. A. Barnes, *J. Non-Newtonian Fluid Mech.* **1997**, *70*, 1.
[39] D. E. Discher, P. Janmey, Y. L. Wang, *Science* **2005**, *310*, 1139.
[40] T. Yeung, P. C. Georges, L. A. Flanagan, B. Marg, M. Ortiz, M. Funaki, N. Zahir, W. Y. Ming, V. Weaver, P. A. Janmey, *Cell Motil. Cytoskeleton* **2005**, *60*, 24.
[41] B. L. Seal, T. C. Otero, A. Panitch, *Mater. Sci. Eng. R* **2001**, *34*, 147.
[42] G. M. Harbers, K. Emoto, C. Greef, S. W. Metzger, H. N. Woodward, J. J. Mascali, D. W. Grainger, M. J. Lochhead, *Chem. Mater.* **2007**, *19*, 4405.